applied sciences

MDPI

Article

Potential of Onshore Wind Turbine Inertia in Decarbonising the Future Irish Energy System

Henning Thiesen * and Clemens Jauch

Wind Energy Technology Institute (WETI), Flensburg University of Applied Sciences, 24943 Flensburg, Germany; clemens.jauch@hs-flensburg.de

* Correspondence: henning.thiesen@hs-flensburg.de

Abstract: Power system inertia is an essential part for grid frequency stability and decreases due to the replacement of fossil fuel fired power plants with variable renewable energy sources. This development is not represented sufficiently in unit commitment and economic dispatch models. If considered at all, only synchronous inertia from fossil fuel driven power plants is modelled. This results in increased CO_2 emissions, curtailed renewable energy and high system costs. While wind turbines are a source for synthetic inertia and an important renewable energy source, their capability to provide inertia is not incorporated into energy system models. The work at hand closes this research gap and applies a methodology to depict synthetic inertia provided by wind turbines as part of the optimisation dispatch model. A unit commitment and economic inertia dispatch model of the the all-Island Irish power system is created. The potential of wind inertia is analysed and quantified by assessing CO_2 emissions, curtailed renewable energy and system costs. Results show that synthetic inertia provided by wind turbines can save up 30.99% of the CO_2 emissions, reduce curtailment by up to 39.90% and reduce system costs by 32.72%.

Keywords: economic dispatch modelling; energy system modelling; power system inertia; renewable energy; synthetic inertia; wind energy

Citation: Thiesen, H.; Jauch, C. Potential of Onshore Wind Turbine Inertia in Decarbonising the Future Irish Energy System. *Appl. Sci.* **2022**, *12*, 2984. https://doi.org/10.3390/app12062984

Academic Editor: Maria Vicidomini

Received: 14 February 2022
Accepted: 12 March 2022
Published: 15 March 2022

1. Introduction

To limit global warming, energy systems are decarbonised by replacing fossil fuel driven power plants with renewable energy sources (RESs). Disconnecting synchronously connected generators reduces the overall power system inertia [1]. Inertia is an essential part for power system stability since it limits the speed with which the grid frequency changes, commonly referred to as the rate of change of frequency (ROCOF), and provides time for generators supplying grid frequency control reserves [2]. Frequency converter connected generation units like wind turbines (WTs) and photovoltaic systems (PVs) as well as storage units with the same type of interface to the power system do not provide an inherent inertial response [1]. However, they are able to mimic the behaviour of a synchronously connected rotating mass known as synthetic inertia (SI) [3,4]. Variable speed WTs are a source for SI and as such are already in application [3]. To sustain the controllability of the grid frequency, future power systems will consist of an inherent and a non-inherent inertia part [1].

Some power systems already experience periods with low system inertia during high non-synchronous penetration and/or low power demand [1]. The grid operator of the Hydro-Québec electricity transmission system demanded WTs to support the power system in the same manner as synchronous generators do in terms of an inertial response [5,6]. The all-Island transmission system operator (TSO) from Ireland defines a grid supporting frequency sensitive mode for WTs [7] as well as system operational constraints like an upper limit for non-synchronous penetration, a maximum ROCOF and an operational limit for inertia [8]. The European Network of Transmission System Operators for Electricity

(ENTSO-E) addresses the need for actions in future power systems to compensate the loss of inherent inertia from synchronous generators [9]. However, the requirement for system inertia can be reduced by introducing energy sources with response times faster than traditional mechanical response from conventional generators [10].

Energy system modelling is an important method in aiding energy system analysis [11]. Its main purpose is to assist in designing, planning and implementing future energy systems [12]. Modelling system inertia in energy system models however, is a topic of minor interest. Table 1 sums up the results of a review of relevant literature in which inertia has been considered as part of energy system models. All papers used unit commitment and (economic) dispatch models applying different constraints to account for minimum system inertia, e.g., ROCOF thresholds or grid frequency nadir thresholds. Actual grid islands like Great Britain or the ERCOT power system were analysed or the interconnected Continental European power systems, which as a whole is a synchronous grid island. In conclusion, the review shows that minimum inertia constraints result in increasing system costs, carbon dioxide emissions and curtailed variable RES.

Table 1. Overview of the research highlights, the applied methodology and scenarios, as well as the key results of the reviewed literature.

Author(s)	Research Highlight(s)	Methodology & Scenario	Result(s)
Teng et al. [13]	Introduction of a novel mixed linear integer programming formulation considering frequency constraint formulations, quantification of wind generation uncertainty on inertia and application of a 2030 model of the Great Britain power system	Unit commitment and economic dispatch formulation applying a multi-stage scenario tree. Analysis of increasing ROCOF threshold from 0.5 Hz/ up to 0.2 Hz/s.	A ROCOF threshold of 0.2 Hz/s would lead to extremely high operation cost (120% increase) and wind curtailment (35% increase)
Collins et al. [14]	Enhancement and robustness check of electricity generation of the PRIMES-REF scenario for 2030 EU by quantifying variable RES curtailment, levels of interconnector congestion and electricity prices.	Creating unit commitment and dispatch model using PLEXOS software, integrating a ROCOF limit of 0.75 Hz/s.	Variable RES congestion increase of 11% in Ireland, overall transmission congestion during 24% of the researched time.
Johnson et al. [15]	Filling the knowledge gap of missing inertia modelling in unit commitment and dispatch models	Mixed integer linear programming model created by PLEXOS optimising for least costs. A system inertia constraint is added to the model for stable grid operations.	Increased dispatch costs by $85 million
Mehigan et al. [16]	Analysing the effect of two different levels of the maximum ROCOF threshold (0.5 Hz/s and 1 Hz/s) on curtailment of variable RES, carbon dioxide emissions and production costs in Europe.	Mixed integer linear programme of a European electricity dispatch system implementing minimum inertia constraints based on ROCOF thresholds.	Increase of generation costs of up to 53.1%, variable RES curtailment increase of 2.15% and CO_2 emission increase of 48.9% for researched system.

None of the reviewed papers and unit commitment and economic dispatch models include SI provision of WTs. Only synchronous inertia is considered. However, it is concluded that "[...] synthetic inertia from wind turbines is believed to play an important role in supporting the frequency performance in the future low carbon power system" [13] as well as that "As grids integrate more renewable energy, relying on the current method

of delivering inertia will see escalating costs, which demonstrates the value of integrating new sources of inertia, like synthetic inertia from wind turbines [...]" [15].

The purpose of this work is to close this research gap of unit commitment and economic dispatch models not considering SI provided by WTs and thereby overestimating system costs, RES curtailment and CO_2 emissions. Therefore, a methodology of a unit commitment and economic inertia dispatch model to represent the all-Island Irish power system is applied. A parameter, which determines the SI provision by WTs is analysed as well as two ROCOF thresholds. The potential of wind inertia is quantified by assessing the total CO_2 emissions, RES curtailment and resulting system costs. Other problems related to the increasing penetration of inverter connected units like reactive support, harmonics or black start capability are not researched as these topics are not primarily related to grid frequency stability. The future Irish power systems is analysed in this work, because the present all-Island Irish power system is already characterised by times of a high shares of frequency inverter connected penetration [17]. Such high penetration times occur due to the fact of Ireland being a island with HVDV grid connection to Great Britain as well as a large number of WTs installed. Thus, feed-in from WTs is already curtailed in times of high frequency converter penetration and low system inertia [17]. The Irish grid operator already has reduced the needed system inertia to a minimum [8], requires generation units to provided a fast reacting frequency response [7] and defines an upper limit for non-synchronous penetration and a maximum ROCOF [8].

The following Section 2 provides an overview of the applied methodology. Section 3 describes scenarios and data of the Irish dispatch model. In Section 4 results are summed up and Section 5 concludes the work at hand.

2. Methodology

The introduced methods to depict inertia as part of the energy system dispatch, to provide SI with WTs and incorporated inertia constraints are elaborated in this section. The methodology is incorporated into an open source modelling tool which is presented too. Prior, fundamental basics of inertia provision are introduced.

2.1. Synchronous and Synthetic Inertia in Power Systems

In AC-power systems, power generation and power consumption have to be balanced at all times [2]. The indicator for power balance is the grid frequency, f_{grid} [2]. A power imbalance leads to a deviation of the grid frequency from its nominal value [2]. The speed with which the grid frequency changes is dominated by power system inertia [1]. Equation (1) illustrates this relationship where $\delta f / \delta t$ is the ROCOF, P_{gen} the accumulated power generation, P_{load} the accumulated power consumption and J_{sys} is the overall power system inertia, i.e., the sum of the moment of inertia of all synchronously connected machines [1].

$$\frac{\delta f}{\delta t} = \frac{P_{gen} - P_{load}}{4 \cdot \pi^2 \cdot f_{grid} \cdot J_{sys}} \tag{1}$$

It is state-of-the-art to describe the inertia of a synchronously connected machine with the inertia constant, H_g. The inertia constant represents the proportional expression of the units stored kinetic energy, $E_{g,kin}$, with respect to its apparent power rating, S_g, as depicted in Equation (2) [1,3]. The inertia constant represents the theoretical time, e.g., a synchronous generator, is able to provide its rated power solely using its stored kinetic energy [1]. Likewise, the resilience of a power system against power imbalances can be described with the power system inertia constant [1].

$$H_g = \frac{E_{g,kin}}{S_g} \tag{2}$$

Frequency converter connected generation sources or energy storage units are able to emulate the behaviour of a synchronous generator in the event of a power imbalance

known as synthetic inertia (SI) [3,4]. A common strategy to substitute inertia with WTs is to change the electric power output based on the ROCOF and the frequency [3]. Due to the modified power output, the rotational speed of the WT changes [18]. That might cause the WT to operate at non-optimal rotational speed [18]. In the worst case, the WT disconnects from the system due to over- or underspeed protection while providing SI [19]. Thus, the SI support as well as the non-inertia related power feed-in of the WT is lost [19]. Hence, from the TSO's point of view, the situation changes for the worse. To counteract such problems, a novel control methodology to emulate inertia with WTs is introduced by Gloe et al. [19]. The authors propose to scale the inertia constant with the actual operating point of the WT, considering the cut-in speed and the rated speed of the WT as supporting points [19]. Thereby, the risk of disconnecting the WT while providing inertia is diminished. The variable inertia constant is normalised such that the inertia constant demanded by the TSO, H_{dem}, is provided at rated speed. H_{dem} is determined by the TSO and based on power system requirements. Equation (3) depicts how the provided SI of a WT is calculated were $\omega_{actual,WT}$ is the actual rotational speed of the WT, $\omega_{rated,WT}$ is the rated speed of the WT and $\omega_{cut\_in,WT}$ the cut-in wind speed of the WT.

$$\frac{H_{var}}{H_{dem}} = \frac{0.5 \cdot J_{WT} \cdot (\omega^2_{actual,WT} - \omega^2_{cut-in,WT})}{0.5 \cdot J_{WT} \cdot (\omega^2_{rated,WT} - \omega^2_{cut-in,WT})} \tag{3}$$

SI is not a direct substitution of synchronous inertia since it is not an inherent inertial response [3]. Hence, in future power systems, the overall system inertia constant comprises an inherent and and non-inherent term as depicted in Equation (4).

$$H_{sys} = \frac{\overbrace{\sum_g H_{g,sync} \cdot S_{g,sync}}^{\text{system synchronous inertia}}}{\sum_g S_g} + \frac{\overbrace{\sum_g H_{g,synt} \cdot S_{g,synt}}^{\text{system synthetic inertia}}}{\sum_g S_g} \tag{4}$$

2.2. Dispatch Model Formulation

The hereafter presented methods are created applying the novel modelling tool Open Inertia Modelling (OpInMod) [20]. OpInMod is an open source modelling tool extending the basic functionalites of the open energy modeling framework (oemof) package solph [21,22]. oemof is developed considering a strict open source and non-proprietary philosophy and is implemented in python [21]. Thus, scientific principles like reproducibility are transparency fulfilled [23–26]. Additionally, comparing oemof to the proprietary software solutions which have been applied in the reviewed literature [13–16], its free of charge availability makes it easy to access [21].

In general, oemof, and therefore OpInMod as well, allows for an easy representation of energy systems applying a graph structure consisting of buses and components [21]. Components are used to represent power plants, variable RES units or energy storage units in an energy system model [21]. Buses and components are connected via edges representing an energy flow [21]. Components hold basic attributes of the represented energy system component. For example, a representation of a power plant would hold attributes such as the variable costs, the installed capacity or the power plants efficiency. OpInMod extends oemof.solph functionality to depict different sources of inertia as well as creating additional constraints when modelling system inertia. The before example of a power plant representation would in OpInMod be extended by attributes such as the type of inertia source (synchronous inertia or SI), the generators inertia constant or costs associated with the provision of inertia. OpInMod is published under MIT License and available via Github [27] and zenodo [28]

Figure 1 provides an schematic overview of the modelling process of a unit commitment and economic inertia dispatch model created with OpInMod. The process can be devided in three sub processes. In the first sub process, named preperation and initialisa-

tion, all packages needed are imported as well as the input files. Next, the energy system is created, using components and buses. In the modelling sub process the energy system representation is translated into an optmisation problem, including all sets of constraints, based on python's optmisation package pyomo [29]. The optimisation problem is solved by a freely selectable solver. In Figure 1 the COIN OR (CBC) solver, GNU Linear Programming Kit (GLPK) solver or gurobi solver are listed as examples. The post processing step of the solver results is the last in the modelling sub process. In the third and last sub process, the results are exported and can be further analysed.

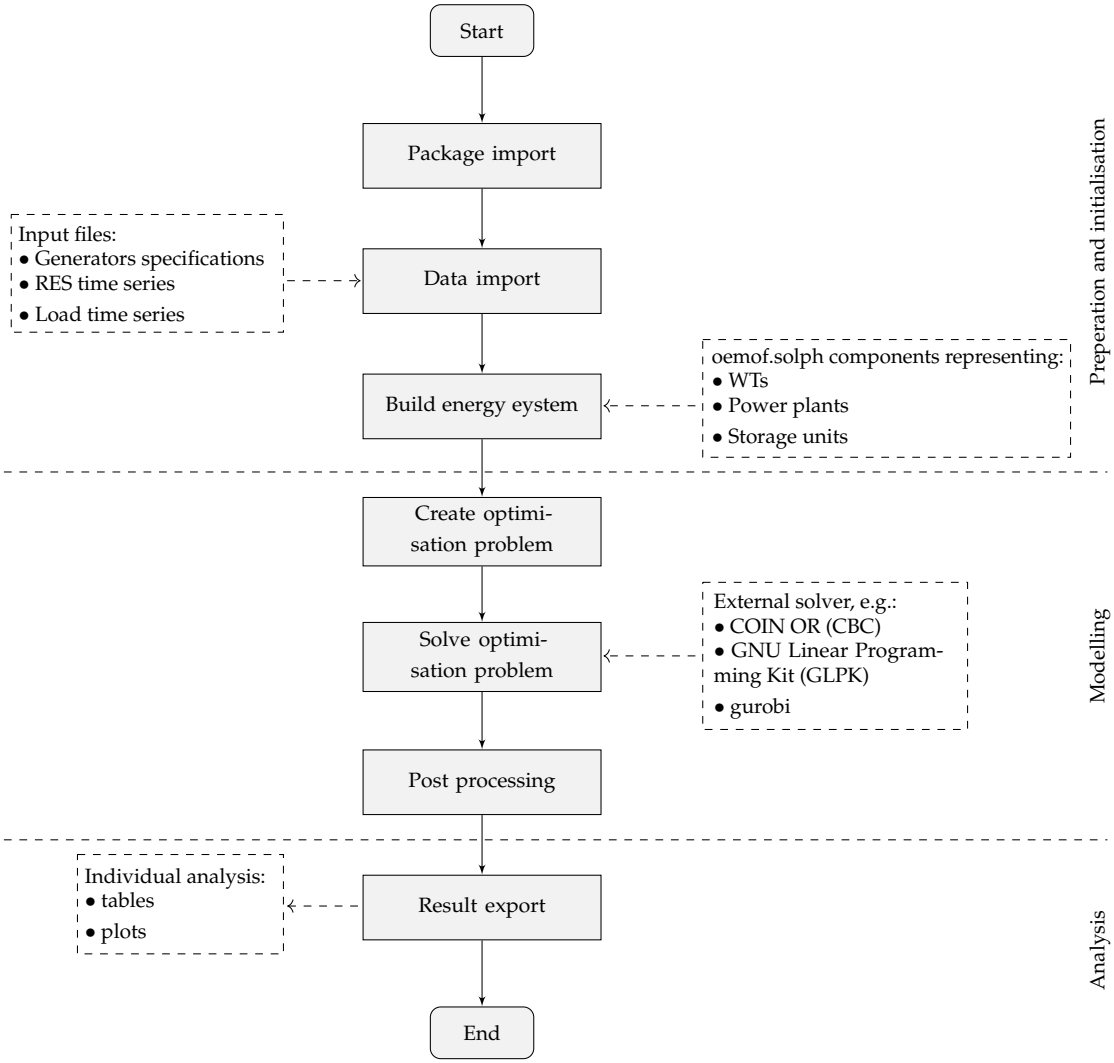

Figure 1. Schematic overview of the full modelling process applying OpInMod. In the preperation and initialisation part of the process, necessary data is imported and the energy system is created using oemof.solph's base components. The base components are extended by attributes and functions to depict synchronous and SI. In the modelling part of the process the optimisation problem, including OpInMod's inertia constraints, is created, solved by an external solver and the results are processed and prepared for the output. In the last section of the process, results are exported and can be further analysed as needed.

The optimisation function depicted in Equation (5) and created by OpInMod is set to minimise the overall system costs subjected to supply power demand for each time step. The first term describes the flow costs by the variable costs of the generator, c_g^{vc} and the flow variable, x_g^{flow} [22]. The second term of the function describes the inertia related costs. The generators moment of inertia is represented by $x_g^{inertia}$, the costs of the generator

providing inertia by c_g^{ic}. Traditionally, a synchronously connected rotating mass provides its full inertia to the power system as long as it is connected. This is reflected by the binary variable $x_g^{source\_inertia}$.

$$\min : \sum_t \sum_g \overbrace{c_g^{vc} \cdot x_g^{flow}(t)}^{\text{costs flow}} + \overbrace{x_g^{source\_inertia} \cdot c_g^{ic} \cdot x_g^{inertia}(t)}^{\text{costs inertia}} \tag{5}$$

2.3. System Inertia Constraints

The optimisation function is bound to two constraints introduced by OpInMod representing the need for minimum system synchronous inertia and minimum overall system inertia. Further constraints inherited from oemof.solph are not presented hereafter but described in [21,22,30]. The minimum system synchronous inertia constraint is depicted in Inequation (6), where $x^{min\_sys\_sync\_inertia}$ is the minimum system synchronous inertia and the right side of the equation is the accumulated moment of inertia of all synchronously connected generators connected to the power system.

$$x^{min\_sys\_sync\_inertia} \leq \sum_g x_g^{source\_inertia} \cdot x_g^{sync\_inertia} \tag{6}$$

Inequation (7) depicts the minimum overall system inertia constraint formulation. The minimum overall system inertia is represented by $x^{min\_sys\_inertia}$. The right part of Inequation (7) depicts the inertia sum all connected generators providing either synchronous or synthetic inertia.

$$x^{min\_sys\_inertia} \leq \sum_g x_g^{source\_inertia} \cdot (x_g^{sync\_inertia} + x_g^{synt\_inertia}) \tag{7}$$

In this work, inertia is either provided by synchronously connected generators or emulated in the form of SI by WTs. Synchronous inertia is also provided by synchronously connected loads [31,32]. However, load inertia is not incorporated in this work, because research on this topic is still incomplete [31,32] and in future systems more loads will be connected with the electrical grid via grid frequency converters which will further reduce their inertia contribution [31].

2.4. Inertia by Synchronous Generators

Synchronously connected generators are hereafter referred to as synchronous generators. The inertia provision by synchronous generators is bound to two constraints. OpInMod incorporates a minimum stable operation constraint as depicted in Inequation (8). The output of a synchronous generator, x_g^{flow}, has to be larger than the product of the units rated power, $x_g^{rated\_power}$ and its minimum stable operation value, $x_g^{min\_stable\_op}$, in per unit. The units connection status is depicted by $x_g^{source\_inertia}$.

$$x_g^{flow} \geq x_g^{source\_inertia} \cdot x_g^{min\_stable\_op} \cdot x_g^{rated\_power} \tag{8}$$

The second constraint depicted by Inequation (9) determines the connection status of the synchronous generator. Since $x_g^{source\_inertia}$ is binary, the Inequation's right part is a proportional expression of the generator output and its rated power. Hence, if the generators output flow is larger then zero, the generator is connected to the power system, provides its inertia and $x_g^{source\_inertia}$ is set to the numeric value of 1.

$$x_g^{source\_inertia} \geq \frac{x_g^{flow}}{x_g^{rated\_power}} \tag{9}$$

2.5. Synthetic Inertia by Wind Turbines

A simplified approach to provide SI with WTs based on the control concept developed by Gloe et al. [19] is implemented in OpInMod. This approach is visualised in Figure 2. Since the concept is based on the actual operating point of a WT, normalised characteristics of the fully open source NREL 5 MW WT are applied [33]. The WT's input is used to determine corresponding normalised rotational speed of the WT as depicted in the top subplot of Figure 2. Thereafter, this value is used to determine the variable inertia constant, H_{var}, with respect to the demanded inertia constant, H_{dem}, as illustrated by the bottom subplot in Figure 2.

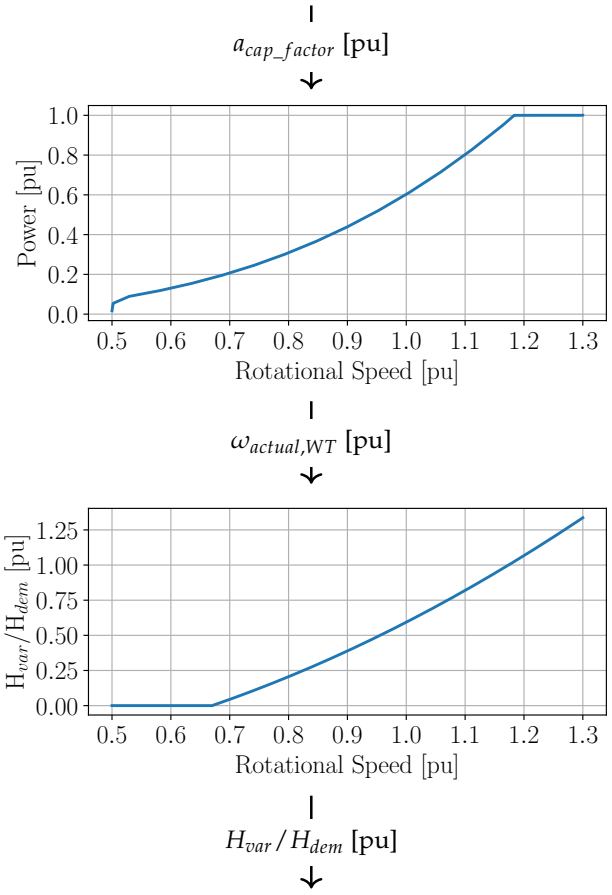

Figure 2. Two step methodology to determine H_{var} / H_{dem} applying the normalised power vs. normalised rotational speed characteristic of the NREL 5 MW WT [34] and the normalised characteristics of the variable H controller [19].

3. Scenario and Data of the Irish Energy Dispatch Model

To assess the potential of wind inertia in the all-Island Irish power system, the before introduced methods are applied to build a unit commitment and economic inertia dispatch model, implementing minimum inertia constraints and SI provided by WTs. Great Britain and France are modelled as well to account for cross border flows with the all-Island Irish system. Since these countries are connected to the Irish system via HVDC interconnectors, inertia is not modelled and these countries are not presented in further detail. However, scenario and data sources for France and Great Britain presented hereafter are the same as for the Irish system.

The scenario applied in this work is based on the 2020 Ten-Year Network Development Plan (TYNDP) of the European Network of Transmission System Operators for Electricity (ENTSO-E) [35,36]. The National Trends (NT) scenario reflects the individual commitments and policies of each single member state to meet CO_2 emission reduction targets. The

influence of the EU is reduced to a minimum in favor of national sovereignty. The power sector in particular experiences a high growth in PV and WT generation. Large scale battery energy storage solutions are limited. Coal fired generation units are replaced by gas-fired and nuclear solutions.

To a large extend, data is provided by the 2020 TYNDP of the ENTSO-E [35,37,38]. Installed capacities per generation type, commodity and emission costs are depicted in Table 2. Characteristics of conventional thermal generators like Operation and Maintenance (O&M) costs, the efficiency and minimum stable operation values are listed in Table 3 [38]. Each generator is assigned with an inertia constant based on literature review [16,39–44]. Feed-in from WTs and PVs is modelled via fixed power factor generation profiles in hourly resolution derived from the Pan-European Climate Database [45]. The WT power factor is also used to determine the variable inertia provided as depicted in Figure 2. Hydro inflow for run-of-river is available in a daily time resolution and on a weekly base for hydro reservoir and open loop pump storage [45]. Such inflow profiles are transformed to hourly profiles.

Table 2. Installed Capacities, commodity and emission costs as well as total energy demands [37].

Type	**Inst. Cap. [MW]**
Wind onshore [MW]	8200
Wind offhore [MW]	5270
Solar PV [MW]	2390
Other RES (e.g., Waste) [MW]	525
Run of river [MW]	238
Natural Gas [MW]	5966
Lignite [MW]	96
Oil [MW]	518
Type	**Costs [EUR/MWh]**
Lignite	3.96
Natural gas	26.316
Light oil	79.92
Heavy oil	61.92
Shale oil	8.28
Biomass	34.89
Other RES (e.g., Waste)	30
CO_2 price [EUR/t]	75.00
Annual demand [TWh]	55.1

Two modelling parameters are varied per optimisation run to assess the influence and potential of SI provided by WTs. First, the demanded inertia constant, H_{dem}, which determines the actual provided SI of WTs [19]. Second, the ROCOF threshold which determines the minimum synchronous system inertia applied to create the constraint depicted in Equation (6) and remaining demand for system SI.

In former grid codes, the TSO of Hydro-Québec requested WTs to emulate a synchronous generator with an inertia constant of 3.5 s and 5 s respectively [5,6]. These two values are applied in this work as well. The Irish grid operator already defines a ROCOF threshold of 1 Hz/s [8]. A 2 Hz/s threshold is considered as well based on recommendations of the ENTSO-E regarding ROCOF withstand capabilities of power generating modules [46]. The resulting minimum synchronous system inertia defined in Equation (6) is calculated by solving Equation (1) for J_{sys}. Therefore, the loss of the largest infeed of 700 MW is used [16]. The overall minimum system inertia applied to create the constraint depicted in Equation (7) is based on system security specifications of Irish TSO. The TSO

defines an operational limit for inertia of 23,000 MWs which can be reformulated as a operational limit for the moment of inertia of 466,077 kg·m^2 [8].

Table 3. Generator characteristics.

Prime Energy	Generator Type	O&M [EUR/MWh]	Efficiency [%]	Min. Stable Op. [%]	CO_2 Emissions [t_{CO_2}/MWh_{el}]	Inertia Constant[s]
Nuclear	-	9.00	33.0	50.0	0.0	5
Hard coal	-	28.68	40.0	43.0	0.8495	3.125
Lignite	-	30.57	40.0	43.0	0.9127	3.5
Natural gas	Conventional old 1	16.49	36.0	35.0	0.5700	4.25
Natural gas	Conventional old 2	16.49	41.0	35.0	0.5005	4.25
Natural gas	CCGT [a] old 1	16.99	40.0	35.0	0.513	4
Natural gas	CCGT old 2	16.99	48.0	35.0	0.4275	4
Natural gas	CCGT present 1	16.99	56.0	30.0	0.3664	4
Natural gas	CCGT present 2	16.99	58.0	30.0	0.3537	4
Natural gas	CCGT new	16.99	58.0	35.0	0.3537	4
Natural gas	OCGT [b] old	16.99	35.0	30.0	0.586	5.25
Natural gas	OCGT new	16.99	42.0	30.0	0.4885	5.25
Light oil	-	22.16	35.0	35.0	0.8022	3.25
Heavy oil	-	24.36	37.5	35.0	0.7524	3.25
Shale oil	-	30.30	29.0	40.0	1.0822	3.5
Biomass	-	10.00	40.0	43.0	0.0	3
Other RES	-	10.00	37.5	35.0	0.0	2

[a] Combined cycle gas turbine (CCGT); [b] Open cycle gas turbine (OCGT).

4. Results

OpInMod provides a large set of results of which system costs, RES penetration, storage units state of charge or cross border flows can be analysed. Since it is the objective of the work at hand to assess the potential of SI provided by WTs, results like the SI provided by WTs itself, RES curtailment, carbon dioxide emissions and system costs will be focused on.

The NT scenario is once optimised without the provision of SI by WTs, only considering inertia provision from synchronously connected generators, representing current state of research and acting as the base scenario in this work. The combination of the two ROCOF threshold parameters (1 Hz/s and 2 Hz/s) and two H_{dem} parameters (3.5 s and 5 s) result in four additional scenarios optimised. All optimisation problems designed with respect to the parameter combinations of the future Irish power system are solvable. Hence, the inertia and power demand constraints are satisfied.

Figures 3 and 4 depict results of a 24 h time series, which is an extract from the whole modelled year. The time series is selected randomly with no specific purpose other then illustrating model functionality, i.e., the influence of inertia constraints on the behaviour and output of dispatchable units. Figure 3 shows results of the base scenario and Figure 4 shows results of the same time period and a ROCOF threshold of 2 Hz/s and a demanded inertia constant of 3.5 s.

The top subplot of Figure 3 illustrates the electric power flow of dispatchable and non-dispatchable units and the bottom subplot the thereof resulting inertia provision. The x-axis shows the time of the day and the y-axis of the top subplot shows the electric power flows, imports and exports in MW and the y-axis of the bottom subplot depicts the provided moment of inertia in kg·m^2. Previous publications depicted the provided inertia represented by the accumulated stored kinetic energy of the connected synchronously rotating masses [15,16,39]. However, since this work incorporates SI provided by WTs and applies the inertia provision methodology introduced by Gloe et al. [19], the stored kinetic energy in the WT's rotor is not a valid representation of the actual provided SI.

Additionally, in future systems inertia should be a tradeable commodity [4]. Therefore, the actual and emulated moment of inertia in kg·m^2 is illustrated.

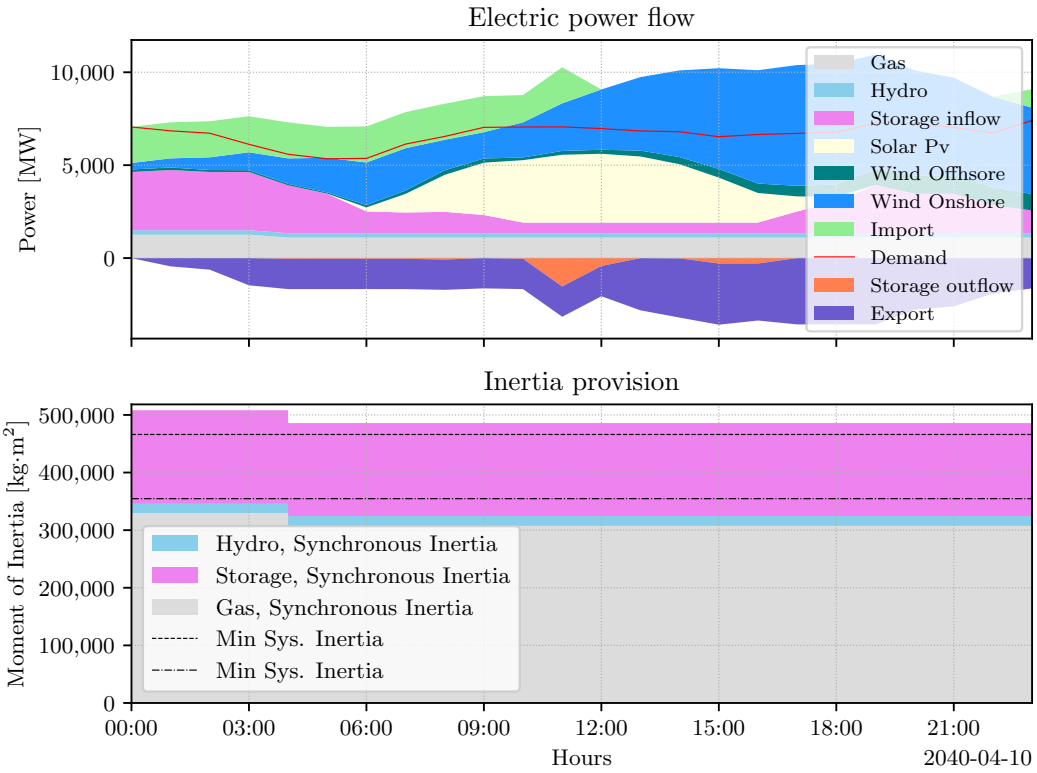

Figure 3. Illustration of a 24 h time series of the base scenario. The top subplot depicts electric power flow results and the bottom subplot flow provided inertia

Figure 3 depicts results of the base scenario. In the top subplot the first six hours of the day are characterised by minor RES feed-in. During these hours, demand is mainly covered by pump storage units, imports, natural gas fired power plants as well as an increasing share of onshore wind feed-in. Electric power flow imports and exports at the same time indicate that the Irish system in this case acts as a transfer system. In other words, electrical energy is transferred from France to Great Britain (or in opposite direction) using the Irish transmission capacities. With increasing onshore wind feed-in, a natural gas fired power plants gets disconnected from the system at a time of 04:00. This results in a downward step in the accumulated provided synchronous inertia by natural gas fired power plants area in the bottom subplot. While feed-in from solar PV and onshore WTs increases during the day and surpasses power demand, feed-in from pump storage units, hydro plants and gas fired power plants remain constant at minimum stable operation due to the minimum stable operation constraint described by Inequation (8). Inertia by such units is needed to satisfy the minimum system inertia constraint described by Inequation (7). Thus, to balance power generation and consumption, power is exported and energy is stored by pump storage units. With decreasing feed-in from solar PV, feed-in from storage units increases. However, since no additional synchronous generator is connected to the power system, provided inertia remains constant throughout the remaining time period. Since feed-in from WTs is high throughout the remaining day and power demand is surpassed by the accumulated feed-in, power exports remain high too.

In conclusion, the before described base scenario demonstrates the influence of the minimum system inertia constraints (see Inequations (6) and (7)). While feed-in from WTs and PV is high throughout the second half of the example time series and surpassing power demand, feed-in from synchronously connected generators such as from gas fired power plants, hydro plants and pump storage units remain at their minimum stable operation

points to provide sufficient inertia. This results in exports and electrical energy being stored in energy storage units.

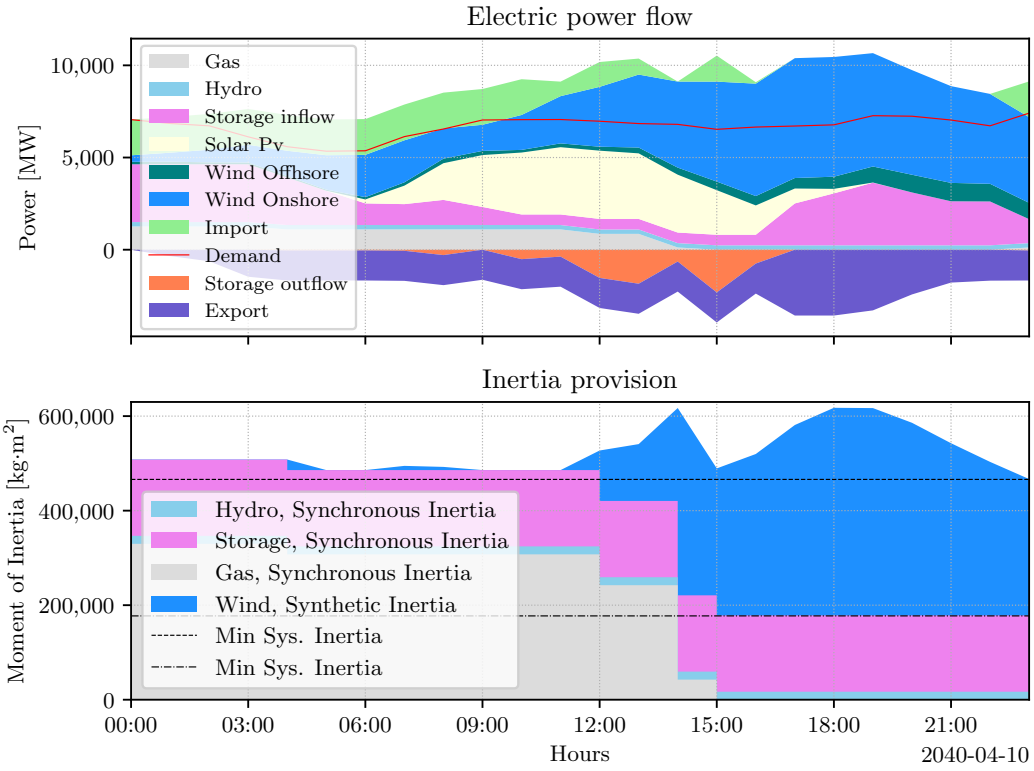

Figure 4. Illustration of a 24 h time series of the parameter combination: ROCOF threshold = 2 Hz/s and demanded inertia constant = 3.5 s. The top subplot depicts electric power flow results and the bottom subplot flow provided inertia.

Figure 4 depicts results of the exact same time period as depicted in Figure 3, but for the parameter combination H_{dem} of 3.5 s and a ROCOF threshold of 2 Hz/s. Hence in this case, WTs provide SI. First 12 h of the time period are almost identical. Minor differences, compared to Figure 3, are visible in the bottom subplot since SI is provided by WTs in the time between 4:00 to 5:00 and 6:00 to 9:00. Moreover, SI provision increases from 11:00 onwards. To satisfy ther overall minimum system inertia constraint (see Inequation (7), natural gas fired power plants, hydro units and pump storage plants are connected to the power system and operate at minimum stable operation. At 12:00 wind SI provision increases significantly. Thus, SI provision from WTs increases. This results in the disconnection of gas fired power plants in the time between 12:00 to 15:00. The system synchronous inertia constraint (see Inequation (6)) is met by the pump storage plants and hydro units provided inertia as well as the provided inertia from gas fired power plants which are disconnected stepwise while feed-in from WTs increases. From 15:00 onwards, the minimum synchronous inertia constraint (see Inequation (6)) can solely be satisfied by the accumulated synchronous inertia from hydro and pump storage plants. Accompanied by sufficient SI from WTs, the overall system inertia constraint (see Inequation (7) is satisfied.

Concluding the model outcome depicted in Figure 4, the beneficial influence of the SI provision by WTs is visible. By the second half of the depicted day, gas fired power plants are completely disconnected from the system, since feed-in from onshore WTs, pump storage units, hydro and offshore WTs is high enough to meet power demand. At the same time, the disconnection of the gas fired power plant is only realisable, due to the fact that overall system inertia constraint is satisfied by the provided wind SI.

Figure 5 illustrates the provided SI (here represented by the synthetic moment of inertia in kg·m^2) by dispatched WTs for the demanded inertia constant (H_{dem}) of 3.5 s and 5 s. The results are illustrated via a histogram plot, where the bars height depicts

the frequency of occurrence and the x-axis depicts the provided SI. The frequency of occurrence is equal to the number of hours of the moddeled year. The green bars depict the synthetic moment of inertia provided by WTs considering the demanded inertia constant (H_{dem}) of 3.5 s and the red bars depict the synthetic moment of inertia provided by WTs considering the demanded inertia constant of 5 s. Obviously, for more then 4300 h of the modelled times series no or very little SI is provided. Thus, for the rest of the modelled time series (the accumulated number of the remaining bars), SI is provided by WT. A higher demanded inertia constant results in higher values for the provided synthetic moment of inertia (compare red bars (H_{dem} = 5 s) to green bars (H_{dem} = 3.5 s)).

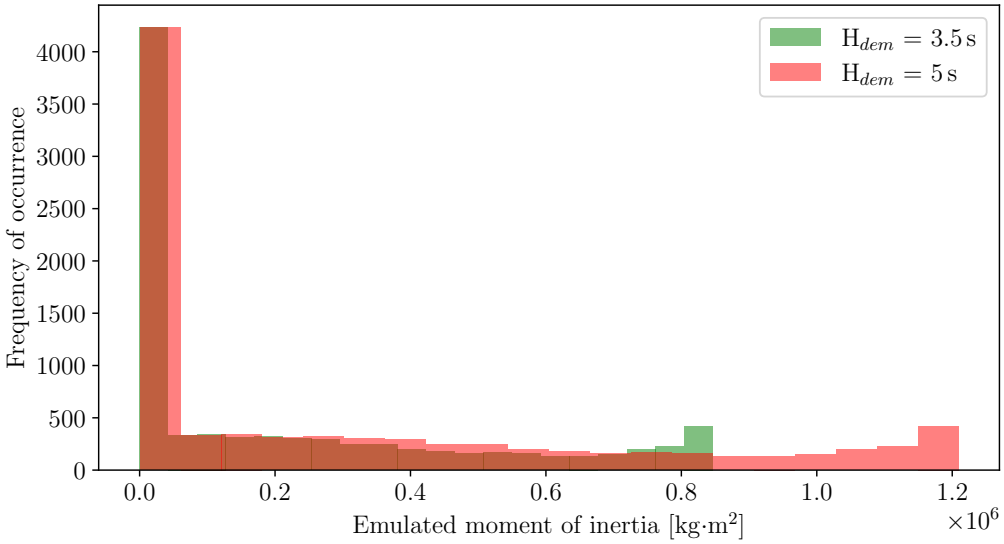

Figure 5. Depiction of the synthetic moment of inertia provided by WTs. The green bars depict the synthetic moment of inertia provided by WTs considering the demanded inertia constant (H_{dem}) of 3.5 s and the red bars depict the synthetic moment of inertia provided by WTs considering the demanded inertia constant of 5 s.

Table 4 shows the accumulated CO_2 emissions and curtailment results per parameter combination. The second column, depicting the CO_2 emissions, indicates that with increasing ROCOF thresholds and higher demanded inertia constants accumulated CO_2 emissions decrease significantly. Equation (10) explains how emission savings in column three of Table 4 are calculated. The respective scenario (e.g., ROCOF = 1 Hz/s, H_{dem} = 3.5 s) results are applied in the numerator of Equation (10). The denominator input is always the result of the base scenario. Increasing the ROCOF threshold up to 2 Hz/s and combining this parameter with an higher H_{dem}, e.g., 5 s, results in CO_2 emission savings of 30.99% with respect to the base scenario. Column four in Table 4 shows accumulated WT and PV curtailment. Similar to the accumulated CO_2 emission results, with increasing demand for WTs to provide SI by higher ROCOF thresholds, the curtailed energy decreases significantly. Equation (11) explains how curtailed energy reduction in column five of Table 4 is calculated. Curtailment reduction up to 39.72% for a demanded inertia constant of 3.5 s and 39.90% for a demanded inertia constant of 39.00% is achievable.

$$reduction\_CO_2\_emissions = \frac{overall\_CO_2\_emissions_{scenario}}{overall\_CO_2\_emissions_{base\_scenario}} \cdot 100 \quad (10)$$

$$reduction\_curtailment = \frac{overall\_curtailed\_energy_{scenario}}{overall\_curtailed\_energy_{base\_scenario}} \cdot 100 \quad (11)$$

Table 4. CO_2 emissions and curtailment results of the analysed scenarios.

Scenario	CO_2 Emissions [t]	Reduction [a] [%]	Curtailment [MWh]	Reduction [a] [%]
Base	4,789,225	0.00	2,613,969	0.00
ROCOF = 1 Hz/s, H_{dem} = 3.5 s	4,085,047	14.70	2,341,290	10.43
ROCOF = 1 Hz/s, H_{dem} = 5 s	4,066,117	15.10	2,341,290	10.43
ROCOF = 2 Hz/s, H_{dem} = 3.5 s	3,474,372	27.45	1,575,412	39.73
ROCOF = 2 Hz/s, H_{dem} = 5 s	3,305,005	30.99	1,570,872	39.90

[a] with respect to the base scenario.

Table 5 shows results of the overall system costs and cost savings with respect to the provided SI. With increasing demand for WTs to provide SI, accumulated system costs decrease significantly, since less feed-in from fossil power plants running at minimum stable operation (must-run capacities) is needed with the purpose to satisfy minimum system inertia constraints. Equation (12) illustrates how cost savings in column two of Table 4 are calculated. Based on the analysed parameter combinations, cost savings up to 32.72% are achievable due to the potential wind inertia provision. The last column of Table 5 depicts the cost savings with respect to the overall provided SI. Increasing the ROCOF threshold parameter and thereby the potential demand for SI results in significantly higher cost savings with respect to the provided SI. Increasing the ROCOF threshold from 1 Hz/s to 2 Hz/s while maintaining the demanded inertia constant at 3.5 s leads to cost savings of 0.09 EURO/kg·m^2 and 0.17 EURO/kg·m^2. Increasing the demanded inertia constant from 3.5 s to 5 s while keeping the ROCOF threshold constant decreases cost savings with respect to the provided SI. While increasing the demanded inertia constant increases system cost saving potential due to SI provision by WTs, the value of the provided SI decreases.

$$reduction\_system\_costs = \frac{overall\_system\_costs_{scenario}}{overall\_system\_costs_{base\_scenario}} \cdot 100 \quad (12)$$

Table 5. Overall system costs and cost savings with respect to the provided SI of the analysed scenarios.

Scenario	System Costs [EURO]	Reduction [a] [%]	Cost Savings [a] for Provided SI [EURO/kg·m^2]
Base	737,265,818	0.00	0.00
ROCOF = 1 Hz/s, H_{dem} = 3.5 s	625,765,315	15.12	0.09
ROCOF = 1 Hz/s, H_{dem} = 5 s	622,733,455	15.53	0.06
ROCOF = 2 Hz/s, H_{dem} = 3.5 s	525,560,884	28.71	0.17
ROCOF = 2 Hz/s, H_{dem} = 5 s	496,034,635	32.72	0.14

[a] with respect to the base scenario.

5. Conclusions

Increasing installed capacities of grid frequency converter connected generation units like WTs and PVs decreases synchronous inertia in energy systems. System inertia is an essential part of grid frequency stability. It limits the instantaneous ROCOF and limits the grid frequency nadir. The trend of decreasing system inertia is not reflected adequately in current unit commitment and economic dispatch models. If inertia in such models is considered at all, only synchronous inertia from fossil power plants is represented. This leads to increased CO_2 emissions, RES curtailment and system costs, since power systems require a minimum system inertia to maintain controllability of the grid frequency. While WTs are a key technology to decarbonise energy systems and a source for an synthetic inertial response, SI is not incorporated into energy system models.

This work closes this research gap. The influence and potential of SI provision by WT on system indicators like CO_2 emissions, variable RES curtailment and system costs is

analysed. Therefore, a methodology to depict SI provision in dispatch optimisation problems is presented. The methodology is incorporated into an open source unit commitment and economic inertia dispatch modelling tool and applied to the all-Island Irish power system. Ireland today is already a power system, in which wind feed-in is curtailed due to low power system inertia and the grid operator has to react by defining an operational level for power system inertia. The model framework OpInMod creates minimum inertia constraints which have to be met by synchronous inertia sources and SI provided by WT. Data and the scenario researched are based on the 2020 TYNDP. Two parameters, the ROCOF threshold determining the needed minimum synchronous system inertia and the demanded inertia constant which determines the provided wind inertia are varied for analysis purpose.

The result analysis shows that the introduction of SI provided by WTs results in the disconnection of fossil fuel fired power plants. The thereof missing inertia is replaced by the provided SI by WTs. Thus, less CO_2 is emitted and costs decrease since WTs are a zero marginal cost source. Based on the analysed parameter combinations, up to 30.99% of the CO_2 emissions can be saved due to the provision of SI by WTs. Curtailment reduction for the parameter combinations show similar results. Curtailment reduction of 39.9% is possible for the parameter combination of a 2 Hz/s ROCOF threshold and a demanded inertia constant of 5 s. Cost savings are in the range of 15.12% and 32.72% with respect to the respective base scenario. System costs saving potential can also be expressed as total cost savings with respect to the overall provided SI by WTs. Here, cost savings are in the range of 0.06 EURO/kg·m^2 and 0.17 EURO/kg·m^2. Increasing the demanded inertia constant and thereby the overall provided inertia reduces the utility for the power system expressed by reduced cost saving per provided inertia.

In total, the analysis shows that incorporating inertia constraints in energy system modelling has a significant influence on the results. Further, SI provided by WTs has a very high potential to reduce CO_2 emissions, RES curtailment and system costs.

Author Contributions: H.T.: Conceptualization, Data curation, Formal analysis, Investigation, Methodology, Software, Validation, Visualization, Writing—original draft & editing. C.J.: Project administration, Resources, Supervision, Writing—review. All authors have read and agreed to the published version of the manuscript.

Funding: This research received no external funding.

Institutional Review Board Statement: Not applicable.

Informed Consent Statement: Not applicable.

Data Availability Statement: The data presented in this study is available in the cited references.

Conflicts of Interest: The authors declare no conflict of interest.

Abbreviations

The following abbreviations are used in this manuscript:

CCGT	Closed cycle gas turbine
ENTSO-E	European Network of Transmission System Operators for Electricity
EU	European Union
MILP	mixed integer linear programming
NT	National Trends
oemof	open energy modeling framework
OCGT	Open cycle gas turbine
OpInMod	Open Inertia Modelling
O&M	Operation and Maintenance
PV	photovoltaic system
RES	renewable energy source
ROCOF	rate of change of frequency

SI	synthetic inertia
TSO	transmission system operator
TYNDP	Ten-Year Network Development Plan
WT	wind turbine

References

1. Tielens, P.; Hertem, D.V. The relevance of inertia in power systems. *Renew. Sustain. Energy Rev.* **2016**, *55*, 999–1009. [CrossRef]
2. Kundur, P.; Balu, N.; Lauby, M. *Power System Stability and Control*; EPRI Power System Engineering Series; McGraw-Hill: New York, NY, USA, 1994; ISBN 978-0-07-035958-1.
3. Fernández-Guillamón, A.; Gómez-Lázaro, E.; Muljadi, E.; Molina-García, A. Power systems with high renewable energy sources: A review of inertia and frequency control strategies over time. *Renew. Sustain. Energy Rev.* **2008**, *115*, 119369. [CrossRef]
4. Thiesen, H.; Jauch, C.; Gloe, A. Design of a System Substituting Today's Inherent Inertia in the European Continental Synchronous Area. *Energies* **2016**, *9*, 582. [CrossRef]
5. Hydro Québec TransÉnergie. Technical Requirements for the Connection of Generation Facilities to the Hydro-Québec Transmission System. Supplementary Requirements for Wind Generation. 2005. Available online: https://www.aeeolica.org/uploads/documents/4535-separata-del-borrador-de-po122.pdf (accessed on 25 May 2020).
6. Hydro Québec TransÉnergie. Transmission Provider Technical Requirements for the Connection of Power Plants to the Hydro–QuéBec Transmission System. 2009. Available online: http://www.hydroquebec.com/transenergie/fr/commerce/pdf/exigence_raccordement_fev_09_en.pdf (accessed on 25 May 2020).
7. EirGrid. EirGrid Grid Code–Version 9. Technical Report. 2020. Available online: https://www.eirgridgroup.com/site-files/library/EirGrid/GridCodeVersion9.pdf (accessed on 21 January 2021).
8. EirGrid and SONI. Operational Constraints Update 21 December 2020. 2020. Available online: https://www.eirgridgroup.com/site-files/library/EirGrid/Operational-Constraints-Update-December-2020.pdf (accessed on 23 March 2021).
9. ENTSO-E. *Need for Synthetic Inertia (SI) for Frequency Regulation*; Report; ENTSO-E: Brussels, Belgium, 2017. Available online: https://consultations.entsoe.eu/system-development/entso-e-connection-codes-implementation-guidance-d-3/user_uploads/igd-need-for-synthetic-inertia.pdf (accessed on 3 May 2019).
10. Denholm, P.; Mai, T.; Wallace Kenyon, R; Kroposki, B.; O'Malley, M. *Inertia and the Power Grid: A Guide without the Spin*; Technical Report NREL/TP-6120-73856; National Renewable Energy Laboratory: Golden, CO, USA, 2020. Available online: https://www.nrel.gov/docs/fy20osti/73856.pdf (accessed on 3 March 2022).
11. Lopion, P.; Markewitz, P.; Robinius, M.; Stolten, D. A review of current challenges and trends in energy systems modeling. *Renew. Sustain. Energy Rev.* **2018**, *9*, 156–166. [CrossRef]
12. Lund, H.; Arler, F.; Østergaard, P.A.; Hvelplund, F.; Connolly, D.; Mathiesen, B.V.; Karnøe, P. Simulation versus Optimisation: Theoretical Positions in Energy System Modelling. *Energies* **2018**, *10*, 840. [CrossRef]
13. Teng, F.; Trovato, V.; Strbac, G. Stochastic Scheduling With Inertia-Dependent Fast Frequency Response Requirements. *IEEE Trans. Power Syst.* **2016**, *31*, 1557–1566. [CrossRef]
14. Collins, S.; Deane, J.; Gallachóir, B.Ó. Adding value to EU energy policy analysis using a multi-model approach with an EU-28 electricity dispatch model. *Energy* **2017**, *130*, 433–447. [CrossRef]
15. Johnson, S.C.; Papageorgiou, D.J.; Mallapragada, D.S.; Deetjen, T.A.; Rhodes, J.D.; Webber, M.E. Evaluating rotational in- ertia as a component of grid reliability with high penetrations of variable renewable energy. *Energy* **2019**, *180*, 258–271. [CrossRef]
16. Mehigan, L.; Al Kez, D.; Collins, S.; Foley, A.; Gallachóir, B.O.; Deane, P. Renewables in the European power system and the impact on system rotational inertia. *Energy* **2020**, *203*, 117776. [CrossRef]
17. EirGrid. All Island Quarterly Wind Dispatch Down Report. 2020. Available online: http://www.eirgridgroup.com/site-files/library/EirGrid/Grid-Code.pdf (accessed on 25 May 2020).
18. Riquelme, E.; Fuentes, C.; Chavez, H.A. A Review of Limitations of Wind Synthetic Inertia Methods. In Proceedings of the 2020 IEEE PES Transmission Distribution Conference and Exhibition—Latin America (T D LA), Montevideo, Uruguay, 28 September–2 October 2020; pp. 1–6. [CrossRef]
19. Gloe, A.; Jauch, C.; Craciun, B.; Winkelmann, J. Continuous provision of synthetic inertia with wind turbines: Implications for the wind turbine and for the grid. *IET Renew. Power Gener.* **2019**, *13*, 668–675. [CrossRef]
20. Thiesen, H. Open Inertia Modelling (OpInMod)—An Open Source Approach to Model Economic Inertia Dispatch in Power Systems. *Preprints* **2022**, 2022010419. [CrossRef]
21. Hilpert, S.; Kaldemeyer, C.; Krien, U.; Günther, S.; Wingenbach, C.; Pleßmann, G. The Open Energy Modelling Framework (oemof)—A new approach to facilitate open science in energy system modelling. *Energy Strategy Rev.* **2018**, *22*, 16–25. [CrossRef]
22. Krien, U.; Schñfeldt, P.; Launer, J.; Hilpert, S.; Kaldemeyer, C.; Pleßmann, G. oemof.solph–A model generator for linear and mixed-integer linear optimisation of energy systems. *Softw. Impacts* **2020**, *6*, 100028. [CrossRef]
23. Bazilian, M.; Rice, A.; Rotich, J.; Howells, M.; DeCarolis, J.; Macmillan, S.; Brooks, C.; Bauer, F.; Liebreich, M. Open source software and crowdsourcing for energy analysis. *Energy Policy* **2017**, *49*, 149–153. [CrossRef]
24. Pfenninger, S.; Hawkes, A.; Keirstead, J. Energy systems modeling for twenty-first century energy challenges. *Renew. Sustain. Energy Rev.* **2014**, *33*, 74–86. [CrossRef]

25. Pfenninger, S.; Hirth, L.; Schlecht, I.; Schmid, E.; Wiese, F.; Brown, T.; Davis, C.; Gidden, M.; Heinrichs, H.; Heuberger, C.; et al. Opening the black box of energy modelling: Strategies and lessons learned. *Energy Strategy Rev.* **2018**, *19*, 63–71. [CrossRef]
26. Wiese, F.; Hilpert, S.; Kaldemeyer, C.; PleßPleßmannmann, G. A qualitative evaluation approach for energy system modelling frameworks. *Energy Sustain. Soc.* **2018**, *8*, 13. [CrossRef]
27. Thiesen, H. Open Inertia Modelling (OpInMod). 2021. Available online: https://github.com/hnnngt/OpInMod (accessed on 19 October 2021).
28. Thiesen, H. Open Inertia Modelling (OpInMod) (0.1). Online. 2021. Available online: http://dx.doi.org/10.5281/zenodo.5582502 (accessed on 19 October 2021). [CrossRef]
29. Hart, W.E.; Watson, J.P.; Woodruff, D.L. Pyomo: Modeling and solving mathematical programs in Python. *Math. Program. Comput.* **2011**, *3*, 219. [CrossRef]
30. Oemof-Developer Group. Open Energy Modelling Framework (oemof), v0.4 GitHub. 2021. Available online: https://github.com/oemof/oemof (accessed on 7 June 2021).
31. Bian, Y.; Wyman-Pain, H.; Li, F.; Bhakar, R.; Mishra, S.; Padhy, N.P. Demand Side Contributions for System Inertia in the GB Power System. *IEEE Trans. Power Syst.* **2018**, *33*, 3521–3530. [CrossRef]
32. Thiesen, H.; Jauch, C. Determining the load inertia contribution from different power consumer groups. *Energies* **2020**, *13*, 1588. [CrossRef]
33. Jonkman, J.; Butterfield, S.; Musial, W.; Scott, G. *Definition of a 5MW Reference Wind Turbine for Offshore System Development*; National Renewable Energy Lab. (NREL): Golden, CO, USA, 2009. [CrossRef]
34. Jauch, C. *First Eigenmodes Simulation Model of a Wind Turbine–for Control Algorithm Design*; TechnicaL Report; WETI: Flensburg, Germany, 2020. [CrossRef]
35. ENTSO-E. TYNDP 2020–Scenario Report. 2020. Available online: https://eepublicdownloads.azureedge.net/tyndp-documents/TYNDP_2020_Joint_Scenario_Report_ENTSOG_ENTSOE_200629_Final.pdf (accessed on 15 March 2021).
36. ENTSO-E. TYNDP 2020–Scenario Building Guidelines. 2020. Available online: https://2020.entsos-tyndp-scenarios.eu/wp-content/uploads/2020/06/TYNDP_2020_Scenario_Building_Guidelines_Final_Report.pdf (accessed on 15 March 2021).
37. ENTSO-E. Data Download. 2020. Available online: https://www.entsos-tyndp2020-scenarios.eu/download-data/#download (accessed on 15 March 2021).
38. ENTSO-E. Unit Data. 2020. Available online: https://www.entsoe.eu/Documents/TYNDP%20documents/TYNDP2018/Scenarios%20Data%20Sets/Input%20Data.xlsx (accessed on 15 March 2021).
39. Trovato, V.; Bialecki, A.; Dallagi, A.A. Unit Commitment With Inertia-Dependent and Multispeed Allocation of Frequency Response Services. *IEEE Trans. Power Syst.* **2019**, *34*, 1537–1548. [CrossRef]
40. Machowski, J.; Lubosny, Z.; Bialek, J.; Bumby, J. *Power System Dynamics: Stability and Control*, 2nd ed.; Wiley: West Sussex, UK, 2020; ISBN 978-1-119-52638-4.
41. Chown, G.; Wright, J.G.; van Heerden, R.; Coker, M. System inertia and Rate of Change of Frequency (RoCoF) with increasing non-synchronous renewable energy penetration. In Proceedings of the 8th Southern Africa Regional Conference 2017, Cape Town, South Africa, 14–17 November 2017.
42. Rawn, B.; Gibescu, M. Effects Future Renewable Installations Will Have on System Synchronous and Synthetic Inertia. Master's Thesis, TU Delft, Delft, The Netherlands, 2012. Available online: https://repository.tudelft.nl/islandora/object/uuid:1c94be1d-3619-40a1-86fa-4a93941ccce50/datastream/OBJ/download (accessed on 15 December 2021).
43. Seneviratne, C.; Ozansoy, C. Frequency response due to a large generator loss with the increasing penetration of wind/PV generation-A literature review. *Renew. Sustain. Energy Rev.* **2016**, *57*, 659–668. [CrossRef]
44. Tielens, P.; Van Hertem, D. Grid Inertia and Frequency Control in Power Systems with High Penetration of Renewables. 2012. Available online: https://lirias.kuleuven.be/retrieve/182648 (accessed on 28 October 2021).
45. ENTSO-E. Pan-European Climate Database. 2020. Available online: https://eepublicdownloads.entsoe.eu/clean-documents/sdc-documents/MAF/2020/Pan-European%20Climate%20Database.7z (accessed on 15 March 2021).
46. ENTSO-E. *Rate of Change of Frequency (RoCoF) Withstand Capability*; Technical Report; ENTSO-E: Brussels, Belgium, 2018. Available online: https://eepublicdownloads.entsoe.eu/clean-documents/Network%20codes%20documents/NC%20RfG/IGD_RoCoF_withstand_capability_final.pdf (accessed on 20 August 2021).